

Supporting information of

Seeds triggered massive synthesis and multi-step room temperature post-processing of silver nano ink — application for paper electronics

Xiao-Yang Zhang^{a, b, c}, *Jia-Jia Xu*^{a, c}, *Jing-Yuan Wu*^{a, c}, *Feng Shan*^{a, c}, *Xiao-Dan Ma*^a, *Yu-Zhang Chen*^a, and *Tong Zhang*^{* a, b, c}

^a *Joint International Research Laboratory of Information Display and Visualization, School of Electronic Science and Engineering, Southeast University, Nanjing, 210096, People's Republic of China.*

^b *Key Laboratory of Micro-Inertial Instrument and Advanced Navigation Technology, Ministry of Education, and School of Instrument Science and Engineering, Southeast University, Nanjing, 210096, People's Republic of China.*

^c *Suzhou Key Laboratory of Metal Nano-Optoelectronic Technology, Suzhou Research Institute of Southeast University, Suzhou, 215123, People's Republic of China.*

Corresponding Author

*Email: tzhang@seu.edu.cn

1. Investigation of the relation between the thickness of the tracks and the printing cycles

The thickness values of the tracks printed were taken from the SEM images, not shown here. We recorded the thickness values at different positions of these tracks printed for different cycles and plotted Figure S1. As shown in this figure, it is clearly that the thickness of the tracks increases linearly with the increasement of the printing cycles. The thickness fluctuation is much more obvious when the number of the printing cycle increases to 10 times. It is because the paper crinkled slightly after too many times re-printing which results to an increasement of the uncertainty of the track thickness after drying. In current study, 2 or 3 times re-printing is suggested as an optimized condition to obtain repeatable silver patterns with high quality which are easy for post-processing.

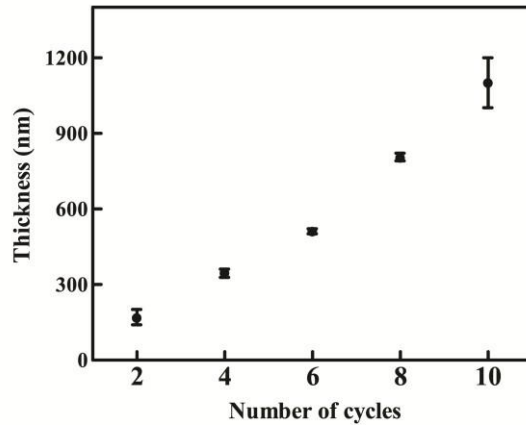


Figure S1. The relation between the thickness of the tracks and the printing cycles. The average values and standard deviation (error bar) were labeled.

2. Characterization of gold seeds used for triggering the reaction of silver nanoparticles synthesis

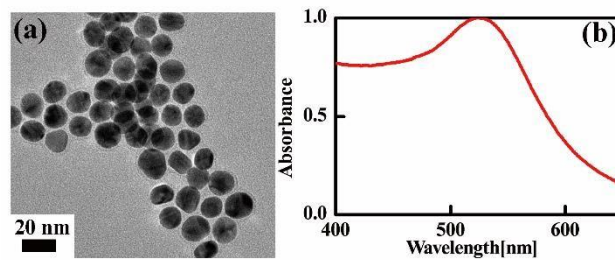


Figure S2. (a) TEM image of gold seeds used for triggering the reaction of silver nanoparticles synthesis. (b) Absorbance spectrum of the gold seed solution.

3. Exhibition of the validity of electroless deposition process using large crystal structure based silver tracks

Figure S3a shows the synthesized silver nanostructures without the addition of H_2O_2 in the initial stage of the reaction. As the types of the seeds in the initial stage of the reaction can not be controlled well, irregular silver crystals with much bigger size were obtained. Apparently, such samples are not suitable for high quality nanoink preparation because the head of the printer are easily be clogged once such big silver crystals are used.

However, the validity of electroless deposition process can be exhibited more clearly by using silver tracks constituted by such big crystals. When large silver crystals were used as ink to print silver tracks, the voids between these nanostructures can be seen clearly as shown in Figure S3 (a).

Note that small nanoparticles were not observed in this SEM image. The printed silver tracks were then treated by MRTP. After one cycle of electroless deposition, the morphology of the silver track had been changed obviously as shown in Figure S3b. Many small nanoparticles were observed, especially in the high resolution SEM image shown in the inset. As no small nanoparticles can be seen in Figure S3a, these small nanoparticles were undoubtedly arising from the silver atoms assembly in the electroless deposition process. These silver atoms absorbed onto the surface of silver nanostructures and filled into the gaps between these adjacent nanostructures as illustrated by the yellow arrows (shown in the inset of Figure S3b). The morphology comparison between Figure S3a and 3b clearly established that small nanoparticles arising from the electroless deposition process can effectively fill into the voids and defects of the silver tracks to improve their conductivity. Meantime, the thickness of the silver tracks did not change obviously.

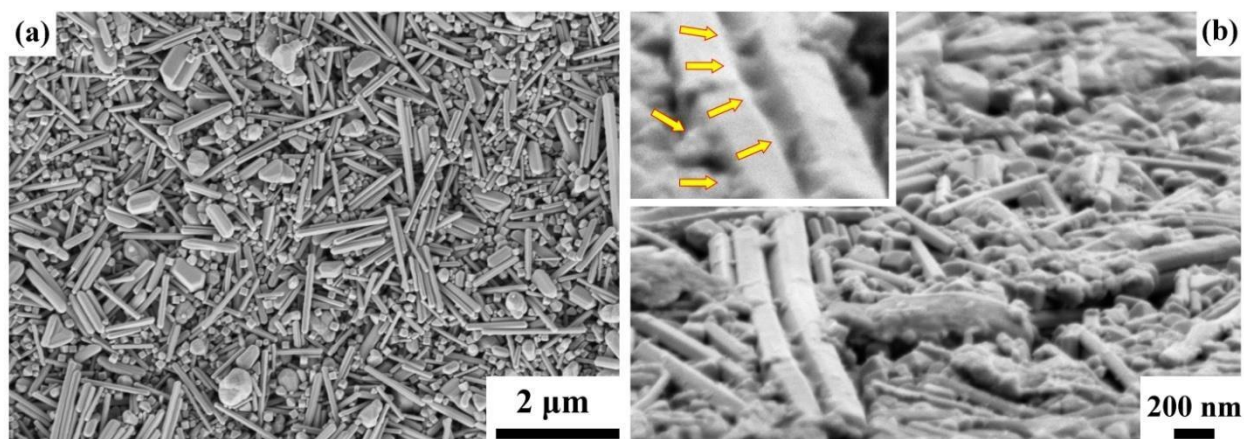


Figure S3. Comparison of the surface morphologies of the silver tracks ink-jet printed using inks containing large crystal structures. (a) shows the SEM image of the as-prepared silver track. (b) shows the SEM images of the silver track treated by one cycle of Step2 of MRTP. The high resolution image shown in the inset illustrated the deposition of small silver nanoparticles on the surface of the large crystal structures.

4. Comparison experiment to exhibit the dissolving ability of acetone for triggering room-temperature sintering of silver nanoparticles

To show the dissolving ability of different organic solvent, we set a comparison experiment using mono-dispersed silver decahedral nanoparticles synthesized as before.¹ The reason we choose silver decahedral nanoparticles is because the shape change and joining behavior of such type of anisotropic silver nanocrystals are easily identified from the absorbance spectral measurement.

Meantime, since the prepared silver decahedral nanoparticles are highly uniform, any morphology changes can be easily observed by TEM imaging.

The experiment is operated by the following steps. First, the as-prepared silver decahedral nanoparticle solution was diluted by water, ethanol and acetone, separately. The volume ration between the new added solvent and the original solution is 2:1. Next, the diluted solutions were centrifuged at 5,000 rpm for ten minutes to deposit the silver decahedral nanoparticles. After the supernatant solution was removed, water was added to dilute and disperse the deposited silver nanoparticles into an appropriate density. Then, the difference among the solutions treated by different solvents is compared. The absorbance spectra of the solutions were measured. Meantime, the morphology changes of the silver nanoparticles were investigated using TEM imaging.

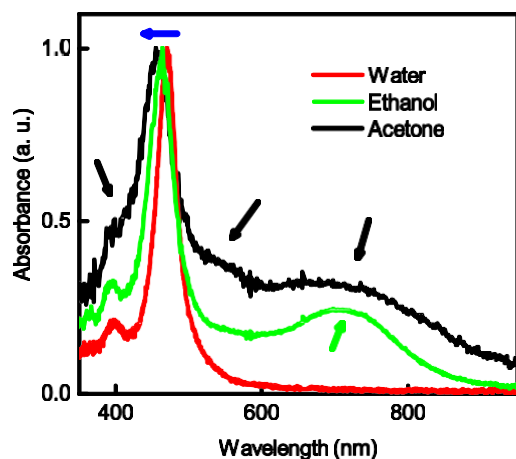


Figure S4. (a) Absorbance spectra of silver decahedral nanoparticles centrifuged in different solvents. Blue arrow illustrates the blue shift of LSPR peak of individual silver decahedral nanoparticles. Green arrow illustrates the emergence of the LSPR band at long wavelength corresponding to the dense self-assembly of silver decahedral nanoparticles after centrifugation in ethanol. Black arrows illustrate the spectral change of nanoparticles after centrifugation in acetone.

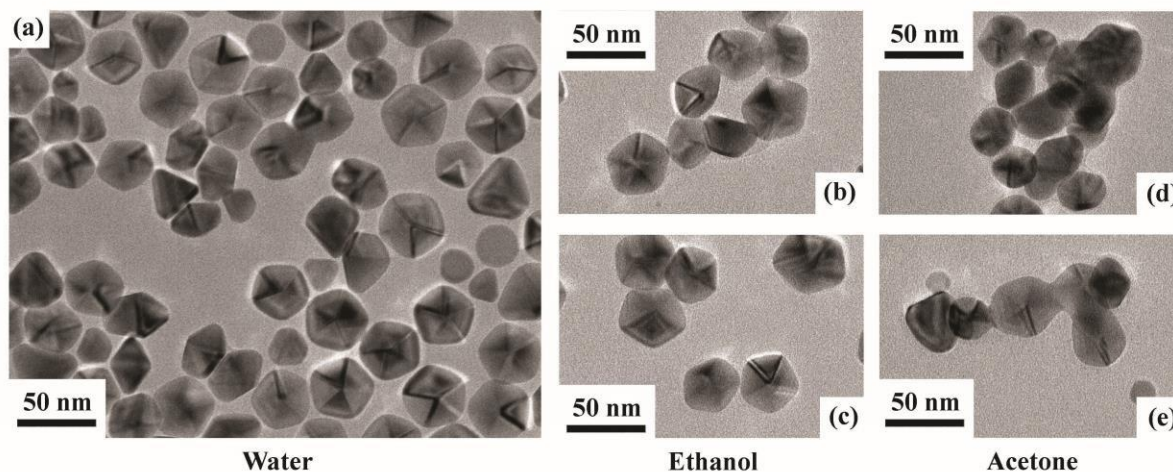


Figure S5. TEM images of silver decahedral nanoparticles centrifuged in (a) ultra-pure water, (b) and (c) in ethanol, (d) and (e) in acetone, respectively.

From the absorbance spectral comparison shown in Figure S4 one can see that the nanoparticles centrifuged by water kept their morphologies well because the absorbance spectrum of this sample is coincident with that of the as-prepared solution. The sharp peak at ~ 460 nm corresponds to the LSPR peak of well separated silver decahedral nanoparticles. The TEM image shown in Figure S5a further established the morphologic stability of the silver nanoparticles. The reason that silver nanoparticles kept their morphology is because these nanoparticles had been well protected by the organic capping agent shell after the synthesis process. Here the organic shell surrounding the silver nanoparticles is PVP.¹

When ethanol was used in the centrifugation process, the PVP shells surrounding the silver decahedral nanoparticles were dissolved partially by ethanol. As the shell became thinner, the activity of the silver nanoparticles was enhanced. Therefore, these nanoparticles with enhanced activity were easily assembled to each other leading to a new LSPR band at long wavelength (~ 720 nm) as shown in Figure S4.² However, as shown from the TEM images in Figures S5b and 5c, one can see the morphologies of these silver decahedral nanoparticles were still kept well although they self-assembled closely. It indicated that the PVP shell was not dissolved completely from the surface of the silver nanoparticles when ethanol was used in the centrifugation process.

When acetone was used in the centrifugation process, the PVP shells surrounding the silver decahedral nanoparticles were dissolved completely. The silver decahedral nanoparticles became

active enough to sinter together at room temperature. Meantime, the shape and size of the silver decahedral nanoparticles changed significantly without the protection of the PVP shells. Both the absorbance spectrum in Figure S4 and the TEM images in Figure S5d and 5e established the above explanation clearly. The blue-shift of the main LSRP peak at short wavelength reflected the shape change of the silver decahedral nanoparticles because their corners and tips had disappeared. Irregular nanoparticles occurred obviously. As the room-temperature sintering was triggered by acetone, these nanoparticles randomly joined together, resulting in a wide wavelength range increase seen from the absorbance spectrum.

The above experimental result successfully exhibited the dissolving ability differences between acetone and ethanol. It clearly established the powerful dissolving ability of acetone to trigger room-temperature sintering of silver nanoparticles in Step1 of MRTTP. In addition, it also gave an explanation why the silver nanoparticles can be washed using ethanol in the centrifugation process, and still kept stable in the ink-jet printing process.

5. Illustration of the simulation model using 3D finite element method

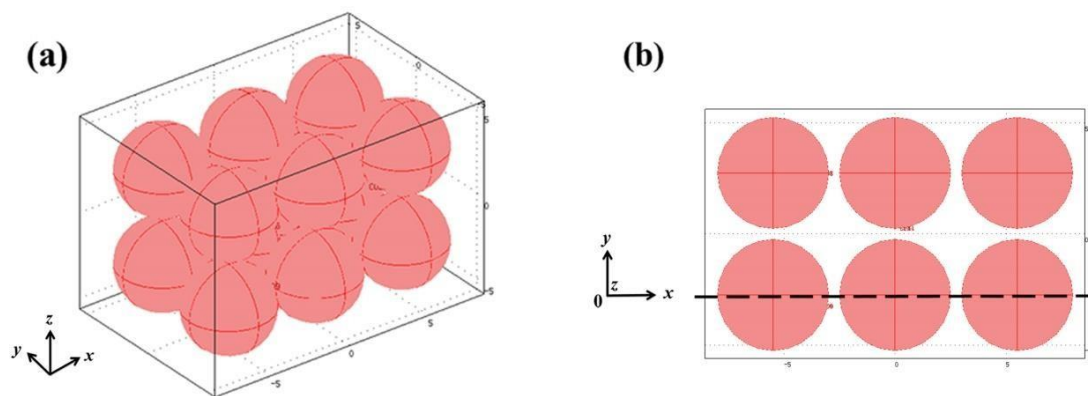


Figure S6. Illustration of the simulation model. (a) shows the distribution of the simulated two layers of silver nanospheres with equal distance of 5 nm from the lateral view section. (b) shows the top view section of the simulated nanospheres. Black dashed lines illustrated the position of the cross section of the electromagnetic field distribution shown in Figure 5a to 5d.

6. Comparison of the technology features of methods reported for printed electronics

Recently, various methods of particle synthesis and post processing processes for printed electronics have been reported. However, the exhibited technology features of these reports are quite different.

As a rapid developing technology, there are still a lot of technique problems needed to be solved. Table S1 listed the main technology features reported by different groups. No.1 listed the result using our optimized ink and MRTP method. No.2 listed the result using our synthesized silver nanostructures without the addition of H₂O₂ (Figure S3). It is clearly that the resistivity of tracks constituted by nanospheres is much lower. In addition, without the filtration step, the print head were blocked seriously using the inks of No.2 after several times printing. This print head blocking problem was not observed when the inks of No.1 was used in our experiments. It indicated that there were very few big particles in the original solution using our H₂O₂ assisted synthesized method. It is therefore an active technology advance meeting the practical demand of ink preparation. The comparison data in the table also indicate that the final resistivity of the tracks is decided by many factors, such as the particle synthesis method, the particle size and the post-processing treatment method. In summary, the main technology features of our proposed method listed in No.1 include fine shape control in large amount, filtration-free and room temperature post-processing which are quite attractive for the paper electronic applications.

Table S1 Technology features reported by different groups

No.	Amount of AgNO ₃	Main particle type	Filtration	Particle size	Post-processing temperature	Resistivity
1	4.5g	Nanospheres	No	~ 45nm and ~ 65 nm	Room temperature	$0.97 \times 10^{-7} \Omega \cdot m$
2	4.5g	Nanowires and nanospheres	No	0.5-2 μm	Room temperature	$5.53 \times 10^{-7} \Omega \cdot m$
Ref 3	10g	Nanospheres	Yes	~ 30 nm	150 °C	$4.7 \times 10^{-8} \Omega \cdot m$
Ref 4	0.85g	Nanospheres	Yes	~ 12 nm	200 °C	$1 \times 10^{-7} \Omega \cdot m$

References:

1. Pietrobon, B.; Kitaev, V. Photochemical Synthesis of Monodisperse Size-Controlled Silver Decahedral Nanoparticles and Their Remarkable Optical Properties. *Chemistry of Materials* **2008**, *20*, 5186–5190.
2. Zhang, X. Y.; Hu, A. M.; Zhang, T.; Lei, W.; Xue, X. J.; Zhou, Y.H.; Duley, W. W. Self-assembly

of Large-scale and Ultrathin Silver Nanoplate Films with Tunable Plasmon Resonance Properties. *ACS Nano* **2011**, *5*, 9082–9092.

3. Huang, Q. J.; Shen, W. F.; Xu, Q. S.; Tan, R. Q.; Song, W. J. Properties of Polyacrylic Acid-coated Silver Nanoparticle Ink for Inkjet Printing Conductive Tracks on Paper with High Conductivity. *Mater. Chem. Phys.* **2014**, *147*, 550–556.

4. Vaseem, M.; Lee, K. M.; Hong, A. R.; Hahn, Y. B. Inkjet printed fractal-connected electrodes with silver nanoparticle ink. *ACS Appl. Mater. Interfaces*, **2012**, *4*, 3300–3307.